2012-10-08

Thioredoxin reductase inhibition elicits Nrf2-mediated responses in Clara cells : implications for oxidant-induced lung injury

Locy, Morgan L; Rogers, Lynette K; Prigge, Justin R; Schmidt, Edward E; Arnér, Elias S J; Tipple, Trent E

Antioxid Redox Signal. 2012 Nov 15;17(10):1407-16.
Mary Ann Liebert
http://doi.org/10.1089/ars.2011.4377
http://hdl.handle.net/10616/41237

ANTIOXIDANTS & REDOX SIGNALING
Volume 17, Number 10, 2012

DOI: 10.1089/ars.2011.4377

ORIGINAL RESEARCH COMMUNICATION

Thioredoxin Reductase Inhibition Elicits Nrf2-Mediated Responses in Clara Cells: Implications for Oxidant-Induced Lung Injury

Morgan L. Locy,[1] Lynette K. Rogers,[1,2] Justin R. Prigge,[3] Edward E. Schmidt,[3] Elias S.J. Arnér,[4] and Trent E. Tipple[1,2]

Abstract

Aims: Pulmonary oxygen toxicity contributes to lung injury in newborn and adult humans. We previously reported that thioredoxin reductase (TrxR1) inhibition with aurothioglucose (ATG) attenuates hyperoxic lung injury in adult mice. The present studies tested the hypothesis that TrxR1 inhibition protects against the effects of hyperoxia via nuclear factor E2-related factor 2 (Nrf2)-dependent mechanisms. ***Results:*** Both pharmacologic and siRNA-mediated TrxR1 inhibition induced robust Nrf2 responses in murine-transformed Clara cells (mtCC). While TrxR1 inhibition did not alter the susceptibility of cells to the effects of hyperoxia, glutathione (GSH) depletion after TrxR1 inhibition markedly enhanced the hyperoxic susceptibility of cultured mtCCs. Finally, *in vivo* data revealed dose-dependent increases in the expression of the Nrf2 target gene NADPH:quinone oxidoreductase 1 (NQO1) in the lungs of ATG-treated adult mice. ***Innovation:*** TrxR1 inhibition activates Nrf2-dependent antioxidant responses in mtCCs *in vitro* and in adult murine lungs *in vivo*, providing a plausible mechanism for the protective effects of TrxR1 inhibition *in vivo*. ***Conclusion:*** GSH-dependent enzyme systems in mtCCs may be of greater importance for protection against hyperoxic exposure than are TrxR-dependent systems. The induction of Nrf2 activation *via* TrxR1 inhibition represents a novel therapeutic strategy that attenuates oxidant-mediated lung injury. Similar expression levels of TrxR1 in newborn and adult mouse or human lungs broaden the potential clinical applicability of the present findings to both neonatal and adult oxidant lung injury. *Antioxid. Redox Signal.* 17, 1407–1416.

Introduction

Pulmonary oxygen toxicity contributes to the development of bronchopulmonary dysplasia (BPD) in premature infants and acute respiratory distress syndrome (ARDS) in children and adults (5,9). Oxygen toxicity is likely mediated through reactive oxygen and nitrogen species produced at higher rates during hyperoxic exposure (3). While the mechanisms responsible for oxygen-induced lung injury have been extensively studied, clinically beneficial therapies are lacking.

Thioredoxin reductase-1 (TrxR1) is a nicotinamide adenine dinucleotide phosphate (NADPH)-dependent oxidoreductase that reduces the active site of cytosolic thioredoxin-1 (Trx1) from the disulfide form to the biologically active dithiol form (1). Trx1 contributes to antioxidant activity by donating electrons to peroxiredoxins for the reduction of hydrogen peroxide (H_2O_2) (28,34), contributes to the synthesis of

Innovation

The present data indicate that thioredoxin reductase-1 (TrxR1) inhibition activates nuclear factor E2-related factor 2 (Nrf2)-dependent antioxidant responses in murine-transformed Clara cells (mtCC) *in vitro* and in adult murine lungs *in vivo*, providing a plausible mechanism for the protective effects of TrxR1 inhibition *in vivo* in an adult murine hyperoxic lung injury model that was previously reported by our group. Furthermore, our data indicate that thioredoxin-1 (Trx1) and TrxR1 are predominantly expressed by ciliated and non-ciliated (Clara) conducting airway epithelial cells in newborn human and newborn murine lungs, which is similar to adult expression; thus broadening the applicability of our findings. Targeted TrxR1 inhibition that elicits Nrf2-dependent antioxidant responses represents a novel clinical therapeutic strategy for preventing or attenuating oxidant-mediated lung injury.

[1]Center for Perinatal Research, The Research Institute at Nationwide Children's Hospital, Columbus, Ohio.
[2]Department of Pediatrics, College of Medicine, The Ohio State University, Columbus, Ohio.
[3]Department of Immunology and Infectious Diseases, Montana State University, Bozeman, Montana.
[4]Division of Biochemistry, Department of Medical Biochemistry and Biophysics, Karolinska Institutet, Stockholm, Sweden.

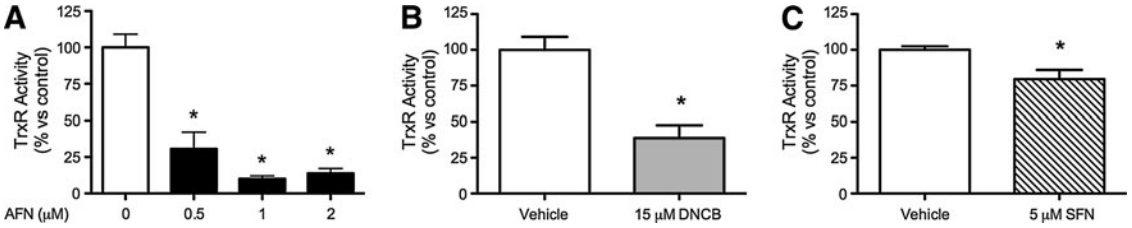

FIG. 1. TrxR1 activities in mtCCs after AFN, DNCB, or SFN treatment for 1 h. (A) AFN treatment decreased TrxR1 activity by approximately 90%; **(B)** DNCB treatment decreased TrxR1 activity by 62%; and **(C)** SFN treatment decreased TrxR1 activity by 21% compared with vehicle-treated controls. Data (mean ± SEM, $n = 3$–4) were analyzed by one-way ANOVA or unpaired *t*-test with significance noted at $p < 0.05$ (*different than vehicle control). AFN, auranofin; ANOVA, analysis of variance; DNCB, dinitrochlorobenzene; mtCC, murine transformed Clara cells; SEM, standard error of the mean; SFN, sulforaphane; TrxR1, thioredoxin reductase-1.

deoxyribonucleotides by donating reducing equivalents to ribonucleotide reductase, is a general intracellular protein disulfide reductant, and regulates the expression of various enzymes and transcription factors (2,16,17). In fetal and adult murine lungs and in adult human lungs, Trx1 and TrxR1 are predominantly expressed in ciliated and non-ciliated (Clara) conducting airway epithelial cells (10,13,23,36).

The induction of antioxidant response genes *via* antioxidant response element (ARE) activation in promoter/enhancer regions of target genes enhances survival from oxidative insults (20,29). ARE activation is primarily mediated by nuclear factor E2-related factor 2 (Nrf2), leading to the increased transcription of genes that provide direct antioxidants, increase glutathione (GSH) levels, and stimulate nicotinamide adenine dinucleotide phosphate synthesis (29). Kelch ECH associating protein-1 (Keap1) controls Nrf2 activation and nuclear accumulation by binding to the Nrf2 protein and targeting it for proteosomal degradation (20). Recent studies suggest that reactive oxygen species mitigate Keap1-mediated Nrf2 degradation via the intermolecular disulfide formation with Cys-151 of Keap1, while a simultaneous disruption of GSH and Trx1/TrxR1 systems causes constitutive Keap1 oxidation and Nrf2 stabilization (12). Furthermore, the genetic ablation of TrxR1 expression in murine hepatocytes (37), in cultured murine embryonic fibroblasts (37), or in murine B-cell lymphomas (25) increases Nrf2-regulated gene induction. Collectively, these data suggest that disruption of the Trx1/TrxR1 system may directly or indirectly influence Nrf2-dependent responses.

Aurothioglucose (ATG) and auranofin (AFN) are anti-inflammatory gold compounds that are clinically used to treat rheumatoid arthritis and experimentally used to inhibit TrxR1 by irreversibly binding its active site selenocysteine (Sec) (14). Experimental models utilize the hyperoxic exposure of newborn or adult mice to investigate the pathogenesis of BPD or ARDS, respectively. In hyperoxia-exposed adult mice, we have previously shown that ATG pretreatment persistently inhibits TrxR1 and attenuates lung edema and inflammation (38). Though the mechanisms responsible for these effects were unclear, our data suggested that TrxR1 inhibition could be therapeutically beneficial in protecting against oxidant-induced lung injury.

The present studies indicate that Trx1 and TrxR1 protein expression is predominantly localized to ciliated and non-ciliated (Clara) epithelia in newborn human and murine lungs, which is similar to fetal and adult lungs. Using murine-transformed Clara cells (mtCC) (24), we tested the hypothesis that TrxR1 inhibition protects against the effects of hyperoxia via Nrf2-dependent mechanisms. TrxR1 inhibition indeed caused rapid Nrf2 nuclear accumulation, increased the transcription of ARE-regulated genes, and increased intracellular GSH levels. Furthermore, our data confirmed that TrxR1 inhibition *in vivo* increased Nrf2 activation in adult murine lungs. While TrxR1 inhibition did not alter the susceptibility of cells to the effects of hyperoxia, GSH depletion after TrxR1 inhibition markedly enhanced the hyperoxic susceptibility of cultured mtCCs. These findings suggest that GSH-dependent enzyme systems in mtCCs may be of greater importance for protection against hyperoxia than are TrxR-dependent

FIG. 2. Nrf2 nuclear abundance and ARE-driven mRNA levels in mtCCs after AFN, DNCB, or SFN treatment and ARE-luciferase activity in mtCCs treated with TrxR1-specific siRNA. (A) Representative Western blot. **(B)** AFN, DNCB, and SFN treatment increased nuclear Nrf2 abundance by 30-fold, 18-fold, and 15-fold, respectively, compared with vehicle-treated controls. Data (mean ± SEM, $n = 5$–8) were normalized to nucleolin and analyzed by one-way ANOVA with Bonferroni *post hoc* with significance noted at $p < 0.05$. (*different than vehicle; $^{\$}$different than AFN). **(C–F)** mtCCs were treated with 1 μM AFN or 15 μM DNCB for 1 h. qRT-PCR analyses indicated greater levels of **(C)** HO-1, **(D)** NQO1, **(E)** TrxR1, and **(F)** GCLM after AFN and DNCB treatment than in vehicle-treated controls. Analyses indicated the independent effects of AFN and DNCB and an interaction between AFN/time and DNCB/time for HO-1, NQO1, TrxR1, and GCLM. dCt values (mean ± SEM, $n = 3$) were analyzed by two-way ANOVA with Bonferroni *post hoc* with significance noted at $p < 0.05$. (*different than same time/vehicle; $^{\%}$different than same time/AFN; $^{\$}$different than same treatment/0 h; $^{\#}$different than same treatment/5 h). **(G)** mtCC were transfected with TrxR1-specific siRNA or empty vector control, ARE-luciferase, and respiratory syncytial virus-β-galactosidase plasmid DNA for 48 h. Luciferase activity was 2.7-fold greater in the TrxR1 siRNA-treated cells than in empty vector-treated controls. Data (mean ± SEM, $n = 9$) were normalized to β-galactosidase and analyzed by an unpaired *t*-test with significance noted at $p < 0.05$ (*different than empty vector control). ARE, antioxidant response element; GCLM, glutamate-cysteine ligase modifier subunit; HO-1, heme oxygenase 1; NQO1, NADPH:quinone oxidoreductase 1; Nrf2, nuclear factor E2-related factor 2; qRT-PCR = quantitative reverse transcriptase–polymerase chain reaction.

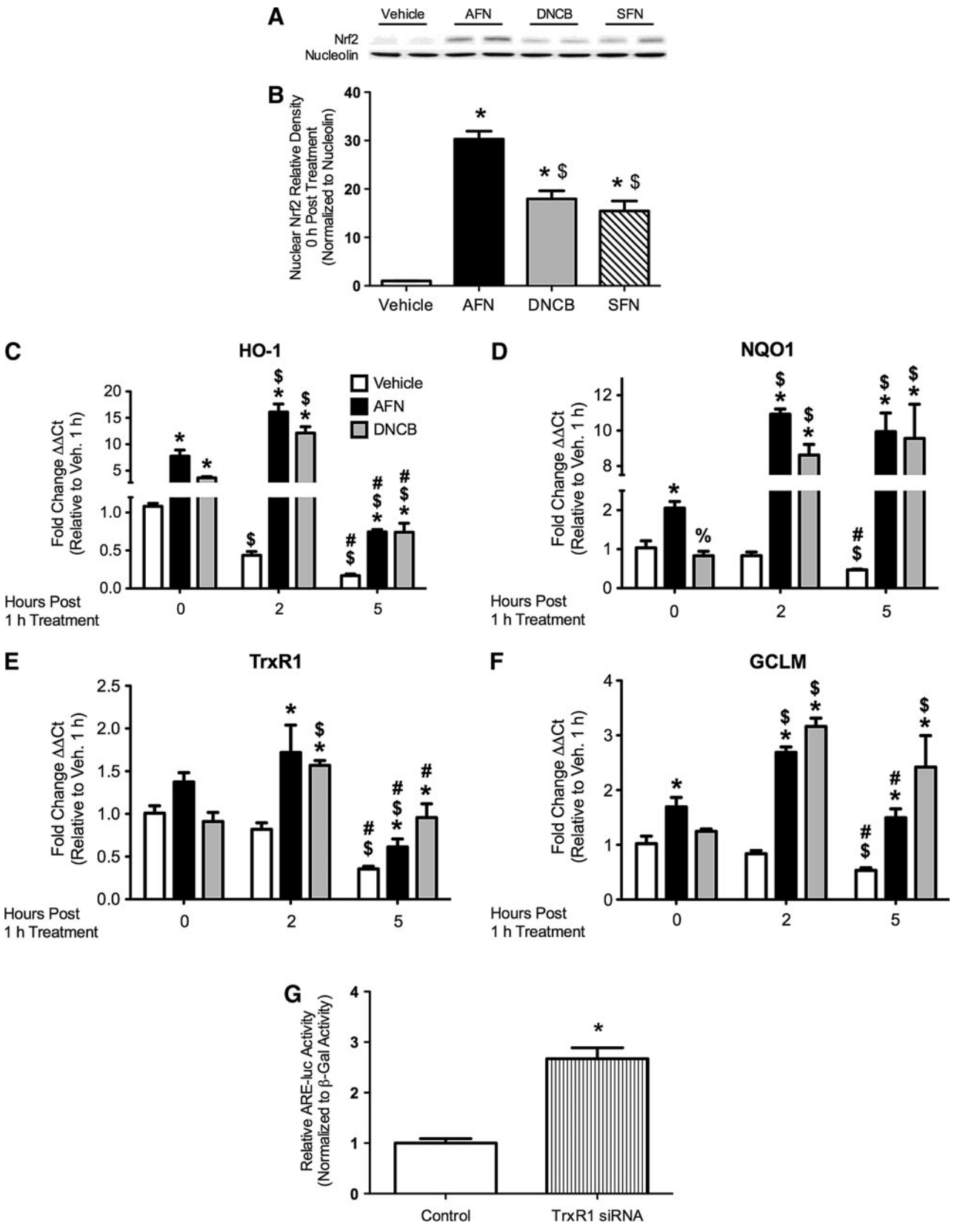
A
Vehicle
AFN
DNCB
SFN
Nrf2
Nucleolin
B
Nuclear Nrf2 Relative Density
0 h Post Treatment
(Normalized to Nucleolin)
Vehicle
AFN
DNCB
SFN
C
HO-1
Vehicle
AFN
DNCB
Fold Change ΔΔCt
(Relative to Veh. 1 h)
Hours Post
1 h Treatment
D
NQO1
E
TrxR1
F
GCLM
G
Relative ARE-luc Activity
(Normalized to β-Gal Activity)
Control
TrxR1 siRNA

systems and that TrxR1 inhibition can upregulate GSH systems above basal levels via Nrf2 activation.

Results

Trx1 and TrxR1 are predominantly expressed in conducting airway epithelial cells in newborn human and murine lungs

Immunohistochemical analyses were performed on sequential lung sections prepared from a single 1 day-old term newborn human or a 1 day-old term newborn mouse to evaluate the expression levels of Trx1 (Supplementary Fig. S1A–D; Supplementary Data are available online at www.liebertpub.com/ars) and TrxR1 (Supplementary Fig. S1E–H) proteins. Trx1 and TrxR1 immunostaining was most intense in both ciliated and non-ciliated airway epithelial cells in newborn human and newborn murine lungs, though the availability of human tissues limited our assessment to one sample. Trx1 and TrxR1 staining in alveolar epithelia was comparatively less intense. This indicated that Trx1 and TrxR1 protein expression was highly enriched in airway epithelia, including lung Clara cell populations.

Selenium supplementation enhances TrxR1 activities

The Sec residue in the TrxR1 C-terminal active site directly contributes to its catalytic function (1). To ensure adequate selenium saturation for TrxR1 synthesis, mtCCs were supplemented with increasing concentrations of selenium (as sodium selenite). Dose-dependent increases in TrxR1 activities in supplemented mtCCs were detected, with TrxR1 activities in mtCCs supplemented with sodium selenite at concentrations above 25 n*M* not being significantly different from each other (Supplementary Fig. S2). Media were, therefore, supplemented with 25 n*M* sodium selenite in all subsequent experiments.

TrxR1 activities are decreased by AFN, dinitrochlorobenzene, and sulforaphane

We previously found that the TrxR1 inhibitor ATG attenuated hyperoxic lung injury in adult mice (38). Therefore, we sought to determine whether Nrf2 activation could be involved by studying the effects of TrxR1 inhibitors AFN and dinitrochlorobenzene (DNCB) and the well-characterized Nrf2 inducer sulforaphane (SFN). Our data revealed that AFN (Fig. 1A), DNCB (Fig. 1B), and sulforaphane (SFN) (Fig. 1C) all significantly decreased TrxR1 activities in mtCC lysates after 1 h treatment. Lysate TrxR1 activities were approximately 90% lower in AFN-treated cells, 62% lower in DNCB-treated cells, and 21% lower in SFN-treated cells than in vehicle-treated controls. Since TrxR1 activities in cells treated with 1 or 2 μM AFN were not significantly different, 1 μM AFN was used for subsequent experiments. TrxR1 activities in AFN-treated mtCCs were not different than in vehicle-treated controls 24 h after AFN treatment for 1 h (data not shown). These data indicate that 1 h treatment of mtCCs with AFN, DNCB, or SFN significantly inhibits TrxR1 activity.

TrxR1 inhibition increases nuclear Nrf2 levels

To determine whether transient TrxR1 inhibition alters Nrf2 responses, Western blot analyses for Nrf2 were performed on nuclear fractions from mtCCs treated with 1 μM AFN, 15 μM DNCB, or 5 μM SFN for 1 h (Fig. 2). AFN, DNCB, and SFN increased nuclear Nrf2 protein levels by 30-, 18-, and 15-fold, respectively, compared with control-treated cells (Fig. 2B). Nuclear Nrf2 protein accumulation was still apparent 2 h post-AFN or DNCB treatment, while levels no longer differed from vehicle-treated controls at 5 h (data not shown).

TrxR1 inhibition increases ARE-mediated gene transcription and intracellular GSH levels

Quantitative reverse transcriptase-mediated polymerase chain reaction (qRT-PCR) was utilized to assess the mRNA levels of ARE-regulated genes after the AFN or DNCB treatment of mtCCs for 1 h. Two-way analysis of variance (ANOVA) indicated the independent effects of AFN and DNCB treatment and time-dependent induction in transcripts of heme oxygenase 1 (HO-1), NADPH:quinone oxidoreductase 1 (NQO1), TrxR1, and glutamate-cysteine ligase modifier subunit (GCLM). In vehicle-treated mtCCs, baseline HO-1, NQO1, TrxR1, and GCLM mRNA levels were ~50% less than the baseline at 5 h (Fig. 2C–F). The HO-1 transcripts were similarly elevated by AFN and DNCB immediately after treatment, further elevated 2 h post-treatment, and returned to baseline levels by 5 h (Fig. 2C). NQO1 transcripts were increased two-fold by AFN immediately after treatment, were elevated by AFN and DNCB 11 and 9-fold, respectively, at 2 h, and remained elevated at 5 h (Fig. 2D). Increases in TrxR1 mRNAs were most pronounced at 2 h after AFN or DNCB treatment (Fig. 2E). In AFN-treated cells, GCLM transcripts were increased two-fold immediately after treatment, three-fold 2 h post-treatment, and returned to baseline at 5 h. DNCB increased GCLM transcripts by 2 h (Fig. 2F).

To determine whether TrxR1 knockdown increases Nrf2-mediated responses, mtCCs were transiently transfected with pU6-m3 control or siTR1-3 plasmids. siTR1-3 robustly knocks down TrxR1 expression in murine lung cells (40). Due to low transfection efficiency (5%–10%), the mtCCs were co-transfected with ARE-driven luciferase plasmids to assess Nrf2 activation. ARE-luciferase promoter activity was 2.7-fold greater in lysates from siTR1-3-treated cells than in pU6-m3-treated controls (Fig. 2G).

TrxR1 inhibition increases total GSH levels in mtCCs in hyperoxia

We determined whether increased GCLM transcription correlated with increased intracellular GSH contents by measuring the total GSH levels in mtCC lysates after treatment with 1 μM AFN or 15 μM DNCB treatment for 1 h (Fig. 3A). Two-way ANOVA indicated the independent effects of AFN and DNCB treatment and interactions between AFN/time and DNCB/time on GSH levels. In DNCB-treated cells, intracellular GSH contents were 72% less immediately after treatment than in vehicle-treated controls; however, at 5 h, the GSH contents were 29% greater. The GSH contents in AFN-treated cells were 33% greater at 5 h. GSH reductase activities in AFN or DNCB-treated cells were not different than in vehicle-treated controls at any time point tested (data not shown).

To determine the effect of hyperoxic exposure on GSH contents, total GSH levels were determined in vehicle, AFN-treated, or SFN-treated mtCCs after exposure to room air

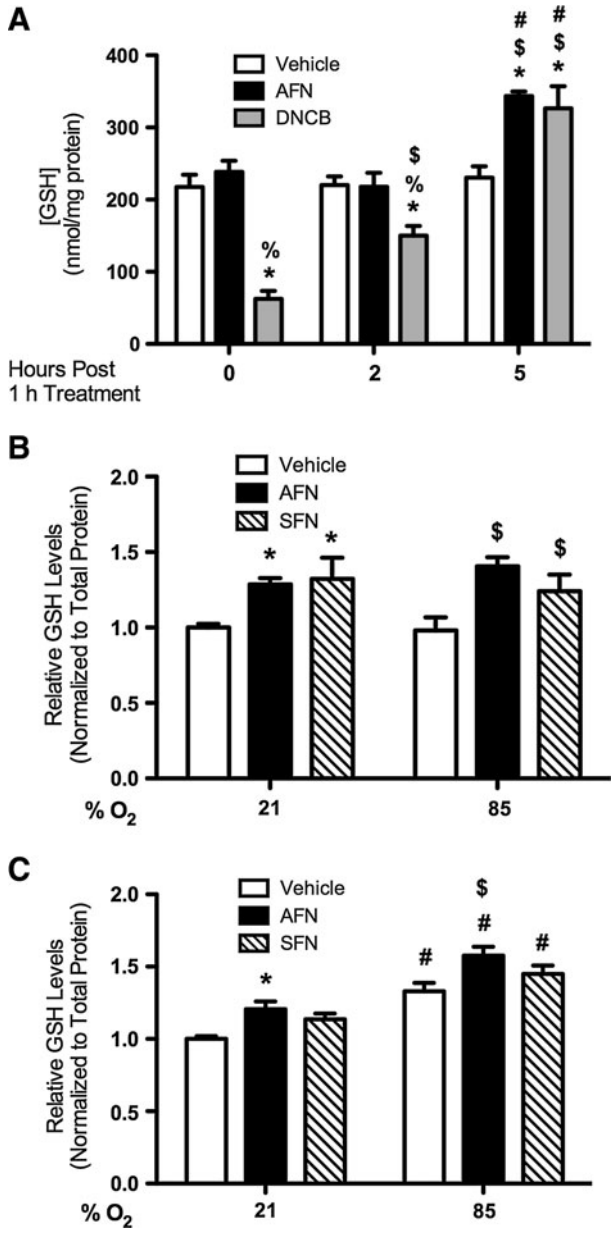

FIG. 3. Total GSH contents in mtCCs after AFN or DNCB treatment and in RA or hyperoxia-exposed mtCCs after AFN or SFN treatment. (A) Total GSH contents were greater in AFN- or DNCB-treated mtCCs 5 h after treatment than in vehicle-treated controls. Analyses indicated the independent effects of and an interaction between treatment and time on GSH levels. Data (mean ± SEM, $n = 6$) were analyzed by two-way ANOVA with Bonferroni *post hoc* with significance noted at $p < 0.05$ (*different than same time/vehicle; $^{\%}$different than same time/AFN; $^{\$}$different than same treatment/0 h; $^{\#}$different than same treatment/2 h). **(B, C)** mtCCs were treated with 1 μM AFN or 5 μM SFN for 1 h, as described in Methods and exposed to RA or hyperoxia for **(B)** 5 h or **(C)** 24 h. Analyses of total GSH levels indicated an independent effect of AFN and SFN treatment at 5 h and the effects of treatment and exposure at 24 h. Data (mean ± SEM, $n = 4$–6) were analyzed by two-way ANOVA with Bonferroni *post hoc* with significance noted at $p < 0.05$ (*different than vehicle/21% O_2; $^{\$}$different than vehicle/85% O_2; $^{\#}$different than same treatment/21% O_2). GSH, glutathione; RA, room air; SFN, sulforaphane.

(21% O_2, RA) or hyperoxia (85% O_2) for 5 or 24 h. Two-way ANOVA indicated independent effects of AFN and SFN treatment on GSH levels at 5 h (Fig. 3B). Hyperoxic exposure for 5 h increased the GSH levels in AFN-treated cells by 31% and in SFN-treated cells by 21% compared with hyperoxia-exposed controls. Two-way ANOVA indicated effects of AFN treatment and exposure and SFN treatment and exposure at 24 h (Fig. 3C). The GSH contents in vehicle-treated hyperoxia-exposed mtCCs were 25% greater at 24 h compared with RA-exposed controls. The GSH levels in hyperoxia-exposed AFN-treated mtCCs were 16% greater than in vehicle-treated controls at 24 h. The SFN-induced increases in GSH levels were comparable to those elicited by AFN treatment.

GSH depletion but not AFN treatment increases the susceptibility of mtCCs to hyperoxic exposure

To determine the effect of transient TrxR1 inhibition on cell viability, mtCCs were treated with 1 μM AFN for 1 h. AFN was removed, the cells were washed, and new media were applied containing vehicle or buthionine sulfoximine (BSO), which inhibits γ-glutamyl cysteine ligase, the rate-limiting step in GSH synthesis (27). After exposure to RA or hyperoxia for 24 h, cell viability was assessed by trypan blue exclusion (Fig. 4A) and ATP contents (Fig. 4B). By trypan blue exclusion, AFN treatment reduced the viable cell numbers in RA by 28%, while no differences in ATP contents were detected. In the analyses of RA-exposed cells, viability was significantly lower in BSO-treated cells than in the vehicle-treated controls, as determined by trypan blue exclusion and was not different than AFN treatment alone. The combination of AFN followed by BSO reduced the viable cell numbers by 89% compared with vehicle-treated controls by trypan blue exclusion (Fig. 4A). Furthermore, the ATP contents after RA exposure were 49% lower in AFN-treated mtCCs treated with BSO than in similarly exposed vehicle-treated controls. In RA, neither AFN treatment nor BSO treatment significantly altered cell numbers compared with vehicle treatment (Fig. 4B).

Hyperoxic exposure decreased viable cell numbers in all treatment groups when compared with corresponding RA control groups, as assessed by trypan blue exclusion (Fig. 4A). AFN treatment alone did not alter viable cell numbers after 24 h of hyperoxic exposure, whereas the addition of BSO to the culture medium after AFN treatment diminished viable cell numbers by greater than 99%. The effect of BSO on cellular ATP contents in hyperoxia revealed similar trends to viability assessments using trypan blue exclusion (Fig. 4B). After hyperoxic exposure, ATP contents were 79% less in the BSO-treated group than in vehicle-treated controls. AFN treatment followed by BSO treatment decreased ATP contents by an additional 9%.

To determine whether hyperoxic exposure, BSO, and/or AFN treatment was associated with loss-of-cellular-membrane integrity, lactate dehydrogenase (LDH) levels in cell media were measured in all treatment groups (Fig. 4C). In RA, the combination of AFN and BSO treatment increased LDH levels by 1.5-fold compared with vehicle-treated controls. Hyperoxic exposure in the presence of BSO increased media LDH levels by 61% and 59%, respectively, when compared with similarly treated RA and hyperoxia-exposed controls. Furthermore, media LDH levels in hyperoxia-exposed mtCCs

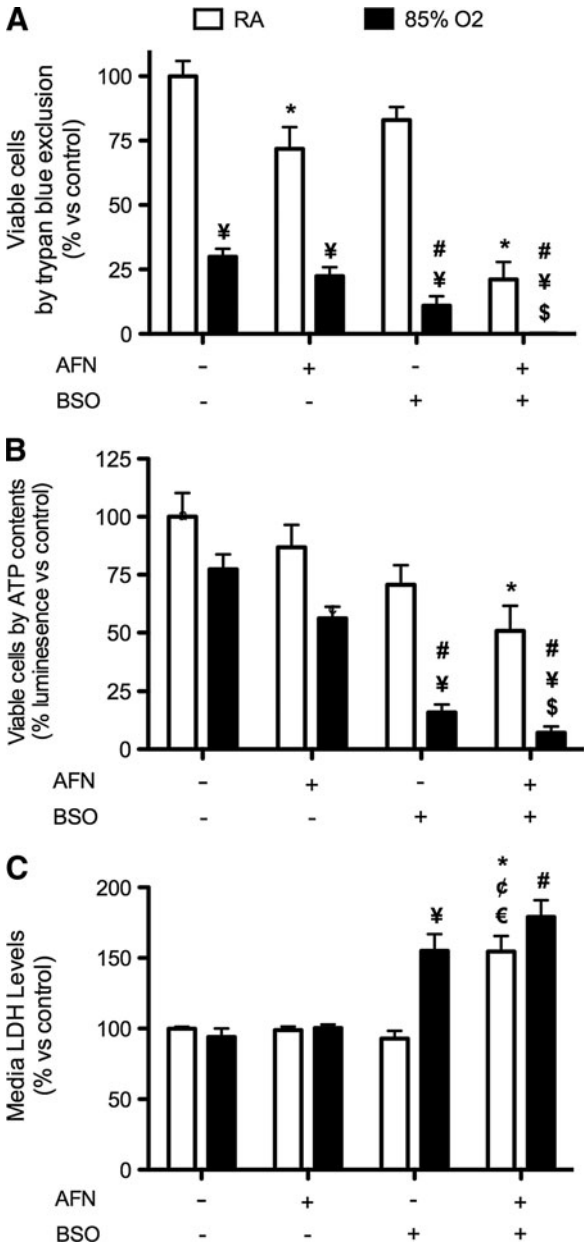

FIG. 4. Viable cell numbers, ATP contents, and media LDH levels after AFN treatment of mtCCs and exposure to RA or hyperoxia for 24 h in the presence or absence of BSO. mtCCs were treated with 1 μM AFN for 1 h, media changed, and subsequently exposed to RA or 85% O_2 for 24 h in the presence or absence of 0.25 m*M* BSO. **(A)** The addition of 0.25 m*M* BSO to the culture medium of AFN-treated cells decreased viable cell numbers in both RA and hyperoxia, as assessed by trypan blue exclusion. **(B)** ATP contents were lower in AFN-treated cells cultured in RA and hyperoxia in the presence of BSO. **(C)** Media LDH levels were greater in AFN-treated mtCCs cultured in RA or hyperoxia than in vehicle-treated mtCCs cultured under similar conditions. Data (mean ± SEM, $n = 9$–12) were analyzed by Kruskal–Wallis followed by Dunn's *post hoc* with significance noted at $p < 0.05$ (*different than vehicle/RA; #different than vehicle/O_2; ¥different than same treatment/RA; $different than AFN/$O_2$; ¢different than AFN/RA; €different than BSO/RA). BSO, buthionine sulfoximine; LDH, lactate dehydrogenase.

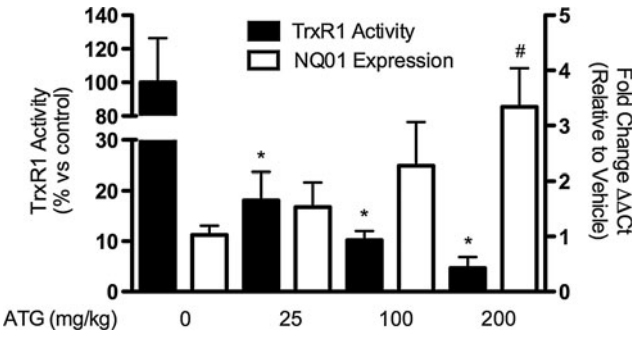

FIG. 5. TrxR1 activities and NQO1 expression in adult murine lungs 24 h after ATG administration. Adult C3H/HeN mice were treated with a single intraperitoneal injection of 0, 25, 100, or 200 mg/kg ATG in saline as described in Materials and Methods. ATG treatment caused dose-dependent decreases in lung TrxR1 activities of approximately 95%. Lung NQO1 mRNA levels were increased by approximately 2.5-fold in ATG-treated mice. Data (mean ± SEM, $n = 3$) were analyzed by two-way ANOVA followed by one-way ANOVA with Bonferroni *post hoc* with significance noted at $p < 0.05$ (*TrxR1 activity different than control; #NQO1 levels different than control). ATG, aurothioglucose.

treated with both AFN and BSO were 90% greater than in hyperoxia-exposed controls.

ATG administration in vivo *increases lung NQO1 expression in adult mice*

To determine whether systemic TrxR1 inhibition by ATG *in vivo* was associated with lung Nrf2 activation, we injected adult C3H/HeN mice with 0, 25, 100, or 200 mg/kg ATG in saline and measured lung TrxR1 activities and NQO1 mRNA levels at 24 h. Compared with controls, lung TrxR1 activities were decreased by 82%, 90%, and 95% after the administration of 25, 100, or 200 mg/kg ATG, respectively (Fig. 5). Furthermore, 25, 100, or 200 mg/kg ATG increased lung NQO1 mRNAs by 0.5, 1.2, and 2.3-fold, respectively, at 24 h. No effect of ATG treatment on total lung GSH levels was detected after 24 h ATG treatment (data not shown).

Discussion

The major findings in the present studies are as follows: (1) TrxR1 inhibition induces Nrf2 responses in mtCCs; (2) SFN inhibits TrxR1 activity in mtCCs; (3) AFN-treated mtCCs are not more susceptible than vehicle-treated cells to the effects of hyperoxia; (4) mtCC viability in hyperoxia is highly dependent on GSH; and (5) ATG treatment *in vivo* inhibits TrxR1 and induces the Nrf2 target gene NQO1 in adult mouse lungs. Our studies also indicate that TrxR1 is highly enriched in newborn human and mouse airway epithelia, though these findings require confirmation in a greater number of samples. The activation of Nrf2-dependent antioxidant responses on TrxR1 inhibition provides a plausible mechanism for our previous findings of attenuated hyperoxic lung injury *in vivo* after the TrxR1 inhibition by ATG (38). We speculate that the protective effects of TrxR1 inhibition on hyperoxia-induced lung injury *in vivo* are likely GSH dependent and mediated *via* Nrf2. Our data also indicate that SFN, a well-described Nrf2 inducer, also inhibits TrxR1, suggesting that TrxR1 inhibition may be a common feature of Nrf2 inducers, as

previously discussed (1). The lack of a protective effect in mtCCs highlights the complexities of investigating cellular redox systems using immortalized cells in isolated culture systems, but their strong GSH dependence is consistent with our proposed model.

AFN was chosen to pharmacologically inhibit TrxR in mtCCs, because it is more stable in solution, requires lower concentrations for complete inhibition (15), and more strongly induces Nrf2/ARE responses *in vitro* than does ATG (19). The transcriptional induction of TrxR1 after 1 h AFN treatment (Fig. 2E) and equivalent TrxR1 activities in AFN-treated and control-treated mtCCs at 24 h suggests the recovery of TrxR1 reductive capacities in mtCCs; likely through the synthesis of new enzyme. This is in contrast to our previous studies *in vivo* in which the long half-life and high level of protein binding by ATG ensured the inhibition of newly synthesized TrxR1 by residual drug (38). We, therefore, speculate that ATG attenuates hyperoxic lung injury *in vivo* by inducing sustained Nrf2-mediated antioxidant responses.

Increased Nrf2-mediated antioxidant responses (Fig. 2C–E), including increased intracellular GSH levels (Fig. 3A), in AFN-treated or DNCB-treated mtCCs are consistent with the recent reports on the constitutive activation of Nrf2-driven antioxidant responses in TrxR1-deficient hepatocytes (37). Furthermore, our data confirm that the treatment of mtCCs with TrxR1-specific siRNA also induces Nrf2-mediated responses (Fig. 2G). While lower GSH levels in mtCCs early after DNCB treatment are likely attributable to DNCB conjugation with GSH catalyzed by glutathione S-transferases (4), sustained increases in GSH levels after AFN or SFN treatment (Fig. 3B, C) are most likely mediated by Nrf2 activation. Keap1 oxidation and Nrf2 stabilization are increased after the simultaneous impairment of Trx1/TrxR1 and GSH pathways in cells, which stably express TrxR1-specific shRNA (12) and in hepatocytes with a genetic defect in TrxR1 expression (37), suggesting that Nrf2 activation can be redox regulated by Trx1/TrxR1 and/or GSH systems. It is likely that the cells in the above-referenced studies adapt to TrxR1 deficiency through the up-regulation of compensatory mechanisms. Our findings demonstrate that compensation for pharmacologically induced TrxR1 deficiency can be rapid.

Nrf2 is integral to pulmonary responses to hyperoxia. It was identified as a candidate gene that regulates hyperoxic lung injury (8) and a *NRF2* promoter polymorphism correlates with increased susceptibility to acute lung injury in humans (26). Conventional Nrf2 knockout mice are more susceptible to hyperoxic lung injury (7) and display impaired resolution of lung injury and inflammation after a nonlethal hyperoxic insult; though GSH administration immediately after the exposure attenuates this damage (30). Clara cell-specific Nrf2 knockout mice exhibit exacerbated hyperoxic lung injury and impaired inflammatory resolution processes during recovery (31), highlighting the importance of Clara cells in pulmonary responses to hyperoxia. 2-cyano-3,12-dioxooleana-1,9(11)-dien-28-oyl (CDDO)-imidazole, which disrupts the cytosolic Keap1:Nrf2 interaction, robustly induces lung antioxidant gene expression (39), and intermittent administration of CDDO-imidazole during hyperoxic exposure induces Nrf2 antioxidant responses and attenuates lung injury (32). Collectively, these data indicate important roles for Clara cell-specific Nrf2 signaling during hyperoxic injury and repair, identifying Nrf2 as a promising therapeutic target.

In the current studies, AFN-treated mtCCs were not more susceptible to hyperoxia than controls, despite the significant inhibition of cellular TrxR1 activity. Dramatic decreases in mtCC viability after BSO, but not AFN treatment, implies that GSH is more important than Trx1/TrxR1 in promoting mtCC viability in hyperoxia. The reasons for the discrepancies between our previous *in vivo* finding of attenuated hyperoxic lung injury after ATG treatment (38) and the lack of protection of mtCCs by AFN are likely complex and illustrate the importance of cell-to-cell communication toward hyperoxic lung injury *in vivo* that is not easily replicated in isolated cell-culture systems. Taken together, however, we conclude that the augmentation of GSH systems through Nrf2 activation may protect against oxidant lung injury. If pulmonary Nrf2 activation can be accomplished via drug-mediated TrxR1 inhibition, which seems to be without detrimental effects, then this approach could constitute a novel strategy for attenuating pulmonary oxidant lung injury. Similar expression patterns of Trx1 and TrxR1 proteins in newborn and adult mouse or human lungs broaden the clinical applicability of the present findings to both BPD and ARDS. If successful, such treatments are of crucial clinical importance and, thus, need to be studied further.

Materials and Methods

Immunohistochemistry

Human tissues from an infant who died in the intensive care nursery were processed within 6 h of death under protocols approved by the Institutional Review Board of the Strong Memorial Hospital (Rochester, NY). Animal protocols were approved by the Institutional Animal Care and Use Committee of The Research Institute at Nationwide Children's Hospital. RA-raised 1 day C3H/HeN pups were euthanized using intraperitoneal (i.p.) ketamine/xylazine (150/15 mg/kg). Inflation-fixed lungs (formalin at 20 cm H_2O, 5 min) were paraffin embedded, and sectioned. For Trx1, the slides were incubated for 5 min in 3% H_2O_2 solution to block endogenous peroxidase activity. The slides were then incubated with monoclonal rabbit anti-human Trx1 primary antibody (#2429, Cell Signaling, Danvers, MA; 1:100) followed by biotinylated goat anti-rabbit secondary antibody (BA-1000, Vector Laboratories, Burlingame, CA; 1:200) and were developed using a Vectastain® Elite kit (Vector Laboratories). Antibody binding was visualized with diaminobenzamidine (DAB). For TrxR1, the slides were deparaffinized, rehydrated, heated to 90°C in 100 m*M* sodium citrate, pH 6.0, for 30 min, and cooled to room temperature. The slides were incubated with 1.5% H_2O_2 for 10 min to block endogenous peroxidase activity and were incubated in rabbit anti-mouse TrxR1 antiserum (Dr. Gary Merrill, Oregon State Univeristy; 1:50) followed by horseradish peroxidase-conjugated goat anti-rabbit secondary antibody (#13859.012, Invitrogen, Carlsbad, CA; 1:1200). Antibody binding was visualized with DAB.

Cell culture and treatments

mtCCs (Dr. Franco DeMayo, Baylor University) were cultured in 1 × Dulbecco's modified Eagle's medium with 4.5 g/l glucose, L-glutamine and sodium pyruvate, 10% fetal bovine serum, 1% penicillin-streptomycin (Mediatech, Manassas, VA), and 25 n*M* sodium selenite (Sigma Chemical Co.,

St. Louis, MO), except as indicated in Supplementary Figure S2. The cells were plated at equal densities, allowed to adhere overnight, and treated with dimethyl sulfoxide (Fisher Scientific, Pittsburgh, PA) control, AFN (Sigma), DNCB (Sigma), or SFN (LKT Laboratories, Inc., St. Paul, MN) for 1 h in serum-free media followed by three washes with Dulbecco's phosphate-buffered saline. The cells were either collected or cultured in fresh media without an inhibitor and exposed to RA or 85% O_2 in oxygen-controlled incubators (Biospherix, Lacona, NY). For a subset of experiments, 4 μl/ml of 6.25 m*M* BSO (Sigma, 0.25 m*M* final concentration) or 4 μl/ml Dulbecco's phosphate buffered saline was added to the media after AFN removal.

TrxR1 activities and GSH levels

TrxR1 activities in cell lysates were determined as previously described (6,33). The GSH concentrations of cell lysates were determined as previously described (38).

Nuclear fraction preparation and Western blot

mtCCs treated with AFN, DNCB, or SFN for 1 h were collected and lysed in sucrose buffer (0.32 *M* sucrose, 10 m*M* Tris-HCl, pH 8.0, 3 m*M* $CaCl_2$, 2 m*M* magnesium oxaloacetate, 0.1 m*M* ethylenediaminetetraacetic acid [EDTA], 0.5% Nonidet P-40, 1 m*M* dithiothreitol, and 0.5 m*M* PMSF [phenylmethylsulfonyl fluoride]). Lysates were centrifuged for 5 min at 500 *g* at 4°C, and the supernatant (cytoplasmic fraction) was removed. Nuclei were washed in sucrose buffer without Nonidet P-40 and were centrifuged as just described. After supernatant removal, the nuclear pellet was resuspended in 30 μl of hypotonic buffer (20 m*M* HEPES, pH 7.9, 1.5 m*M* $MgCl_2$, 20 m*M* KCl, 0.2 m*M* EDTA, 25% glycerol (v/v), 0.5 m*M* dithiotreitol [DTT], and 0.5 m*M* PMSF). Hypertonic buffer (30 μl; 20 m*M* HEPES, pH 7.9, 1.5 m*M* $MgCl_2$, 800 m*M* KCl, 0.2 m*M* EDTA, 25% glycerol (v/v), 1% Nonidet P-40, 0.5 m*M* DTT, 0.5 m*M* PMSF, and 4.0 μg/ml each of leupeptin, aprotinin, and pepstatin) was slowly added. Protein concentrations were determined using a Bio-Rad Protein Assay Kit. Samples were separated on 4%–12% bis-tris gels (Invitrogen), transferred to nitrocellulose membranes (iBlot, Invitrogen), blocked with 10% milk/tris-buffered saline containing 1% Tween-20 (TBS-T), and probed using a polyclonal rabbit anti-Nrf2 antibody (H-300, Santa Cruz Biotechnology, Santa Cruz, CA; 1:500) in TBS-T followed by goat anti-rabbit immunoglobulin G-horseradish peroxidase secondary antibody (Bio-Rad, Hercules, CA; 1:12,000) in TBS-T. Membranes were developed using enhanced chemiluminescence (GE Healthcare, Buckinghamshire, UK). As a loading control, membranes were re-probed with polyclonal rabbit anti-nucleolin antibody (ab22758, Abcam, Cambridge, MA; 1 μg/ml).

Quantitative real-time PCR

RNA was isolated from mtCCs or lungs using TRIzol® (Invitrogen) and the RNeasy® Mini Kit (Qiagen, Germantown, MD). cDNAs were synthesized using Oligo d(T) primers, the Superscript® III Reverse Transcriptase Kit (Invitrogen), and dNTPs (Fisher). Primers for murine TrxR1 (18), HO-1 (22), NQO1 (11), GCLM (21), and β-actin (35) (Integrated DNA Technologies, San Diego, CA), SYBR® green/ROX master mix (Superarray, Frederick, MD) and cDNAs were loaded into 96-well plates, and Ct values were obtained using an ABI 7500 Real-time PCR System (Applied Biosystems, Carlsbad, CA). The Ct values were normalized to β-actin. Fold changes were calculated using $2^{(-\mathrm{ddCt})}$.

ARE luciferase analyses

mtCCs were transiently transfected with siTR1-3 or pU6-m3 control plasmid (Dolph Hatfield, NIH), pGL2 (basic) 3xARE Lux (Joan Massague, Memorial Sloan Kettering, Addgene # 14934), and respiratory syncytial virus (RSV)-β-galactosidase (Dr. Y. Liu, Nationwide Children's). Cells were co-transfected at 60% confluence with 12 μg plasmid DNA per well (6 μg 3xARE:RSV-βgal [25:1] and 6 μg of siTR1-3 or control plasmid) on 9.6-cm^2 tissue-culture plates using JetPEI (Polyplus-Transfection) according to the manufacturer's instructions. ARE-luciferase and β-glactosidase activities in cell lysates were determined 48 h after transfection using the Luciferase Reporter Assay System and the β-Galactosidase Enzyme Assay System (Promega), respectively, and a Veritas Microplate Luminometer (Promega).

Cell viability

Viable cell numbers were determined by trypan blue exclusion and by ATP contents by CellTiter-Glo® assay (Promega Corp., Madison, WI). Media LDH levels were determined as follows: 100 μl of test mixture (216 μ*M* nicotinamide adenine dinucleotide (NADH) in 60 m*M* K-phosphate buffer, 0.72 m*M* pyruvate, pH 7.5) was added to 200 μl of the media, and NADH oxidation was recorded at 340 nm for 5 min using a Spectramax M2 (Molecular Devices, Sunnyvale, CA).

ATG administration in vivo

Adult C3H/HeN mice (6–8 weeks, $n = 3$) received single i.p. injections of 0, 25, 100, or 200 mg/kg ATG (Research Diagnostics, Flanders, NJ) in saline and were euthanized 24 h after the injection using i.p. ketamine/xylazine (150/15). Lungs were removed and placed in TRIzol on dry ice. A portion of the left lung was homogenized using TissueLyser II (Qiagen).

Statistical analyses

Data were analyzed using GraphPad Prism® software (La Jolla, CA), were tested for homogeneity of variances, and were log transformed when indicated. Data were analyzed by the unpaired *t*-test, one-way ANOVA, or two-way ANOVA followed by Bonferroni *post hoc*. Nonparametric data were analyzed by Kruskal–Wallis followed by Dunn's *post hoc*. Significance was noted at $p < 0.05$.

Acknowledgments

The authors thank Dr. Gloria Pryhuber and BRINDL (BioRepository for Investigation of Neonatal Diseases of the Lung, University of Rochester, NY; newborn human lung slides), Dr. Gary Merrill (Oregon State University; TrxR1 antiserum), Dr. Franco DeMayo (Baylor University; mtCCs), Dr. Dolph Hatfield (NIH; TrxR1 siRNA plasmid), and Cynthia L. Hill for her expert technical assistance. This work was supported by NIH/NHLBI 5K08HL093365-02 (T.E.T.), the Richard P. and Marie R. Bremer Medical Research Fund, the William H. Davis Endowment for Basic Medical Research

from The Ohio State University Medical Center, and UL1RR025755 from the National Center for Advancing Translational Sciences (T.E.T.). Support was also provided by Karolinska Institutet and The Swedish Cancer Society (E.S.A.), and by the NIH/NCI, the NIH/NIA, and the Montana Agricultural Experiment Station (E.E.S. and J.R.P.). The content is the sole responsibility of the authors and does not necessarily reflect the views of the Davis/Bremer Research Fund, The Ohio State University Medical Center, The National Center for Advancing Translational Sciences, or the National Institutes of Health.

Author Disclosure Statement

The authors declare that no competing financial interests exist.

References

1. Arner ES. Focus on mammalian thioredoxin reductases—important selenoproteins with versatile functions. *Biochim Biophys Acta* 1790: 495–526, 2009.
2. Arner ES and Holmgren A. Physiological functions of thioredoxin and thioredoxin reductase. *Eur J Biochem* 267: 6102–6109, 2000.
3. Auten RL and Davis JM. Oxygen toxicity and reactive oxygen species: the devil is in the details. *Pediatr Res* 66: 121–127, 2009.
4. Awasthi YC, Sharma R, and Singhal SS. Human glutathione S-transferases. *Int J Biochem* 26: 295–308, 1994.
5. Barrios R, Shi ZZ, Kala SV, Wiseman AL, Welty SE, Kala G, Bahler AA, Ou CN, and Lieberman MW. Oxygen-induced pulmonary injury in gamma-glutamyl transpeptidase-deficient mice. *Lung* 179: 319–330, 2001.
6. Cenas N, Prast S, Nivinskas H, Sarlauskas J, and Arner ES. Interactions of nitroaromatic compounds with the mammalian selenoprotein thioredoxin reductase and the relation to induction of apoptosis in human cancer cells. *J Biol Chem* 281: 5593–5603, 2006.
7. Cho HY, Jedlicka AE, Reddy SP, Kensler TW, Yamamoto M, Zhang LY, and Kleeberger SR. Role of NRF2 in protection against hyperoxic lung injury in mice. *Am J Respir Cell Mol Biol* 26: 175–182, 2002.
8. Cho HY, Jedlicka AE, Reddy SP, Zhang LY, Kensler TW, and Kleeberger SR. Linkage analysis of susceptibility to hyperoxia. Nrf2 is a candidate gene. *Am J Respir Cell Mol Biol* 26: 42–51, 2002.
9. Crapo JD. Morphologic changes in pulmonary oxygen toxicity. *Annu Rev Physiol* 48: 721–731, 1986.
10. Dammeyer P and Arner ES. Human protein atlas of redox systems—what can be learnt? *Biochim Biophys Acta* 1810: 111–138, 2011.
11. Dong J, Sulik KK, and Chen SY. Nrf2-mediated transcriptional induction of antioxidant response in mouse embryos exposed to ethanol *in vivo*: implications for the prevention of fetal alcohol spectrum disorders. *Antioxid Redox Signal* 10: 2023–2033, 2008.
12. Fourquet S, Guerois R, Biard D, and Toledano MB. Activation of NRF2 by nitrosative agents and H2O2 involves KEAP1 disulfide formation. *J Biol Chem* 285: 8463–8471, 2010.
13. Godoy JR, Funke M, Ackermann W, Haunhorst P, Oesteritz S, Capani F, Elsasser HP, and Lillig CH. Redox atlas of the mouse. Immunohistochemical detection of glutaredoxin-, peroxiredoxin-, and thioredoxin-family proteins in various tissues of the laboratory mouse. *Biochim Biophys Acta* 1810: 2–92, 2011.
14. Gromer S, Arscott LD, Williams CH, Jr., Schirmer RH, and Becker K. Human placenta thioredoxin reductase. Isolation of the selenoenzyme, steady state kinetics, and inhibition by therapeutic gold compounds. *J Biol Chem* 273: 20096–20101, 1998.
15. Gromer S, Merkle H, Schirmer RH, and Becker K. Human placenta thioredoxin reductase: preparation and inhibitor studies. *Methods Enzymol* 347: 382–394, 2002.
16. Holmgren A. Thioredoxin. *Annu Rev Biochem* 54: 237–271, 1985.
17. Holmgren A. Thioredoxin and glutaredoxin systems. *J Biol Chem* 264: 13963–13966, 1989.
18. Jurado J, Prieto-Alamo MJ, Madrid-Risquez J, and Pueyo C. Absolute gene expression patterns of thioredoxin and glutaredoxin redox systems in mouse. *J Biol Chem* 278: 45546–45554, 2003.
19. Kataoka K, Handa H, and Nishizawa M. Induction of cellular antioxidative stress genes through heterodimeric transcription factor Nrf2/small Maf by antirheumatic gold(I) compounds. *J Biol Chem* 276: 34074–34081, 2001.
20. Kensler TW, Wakabayashi N, and Biswal S. Cell survival responses to environmental stresses via the Keap1-Nrf2-ARE pathway. *Annu Rev Pharmacol Toxicol* 47: 89–116, 2007.
21. Khouzami L, Bourin MC, Christov C, Damy T, Escoubet B, Caramelle P, Perier M, Wahbi K, Meune C, Pavoine C, and Pecker F. Delayed cardiomyopathy in dystrophin deficient mdx mice relies on intrinsic glutathione resource. *Am J Pathol* 177: 1356–1364, 2010.
22. Kim C, Jang JS, Cho MR, Agarawal SR, and Cha YN. Taurine chloramine induces heme oxygenase-1 expression via Nrf2 activation in murine macrophages. *Int Immunopharmacol* 10: 440–446, 2010.
23. Kobayashi M, Nakamura H, Yodoi J, and Shiota K. Immunohistochemical localization of thioredoxin and glutaredoxin in mouse embryos and fetuses. *Antioxid Redox Signal* 2: 653–663, 2000.
24. Magdaleno SM, Wang G, Jackson KJ, Ray MK, Welty S, Costa RH, and DeMayo FJ. Interferon-gamma regulation of Clara cell gene expression: *in vivo* and *in vitro*. *Am J Physiol* 272: L1142–L1151, 1997.
25. Mandal PK, Schneider M, Kolle P, Kuhlencordt P, Forster H, Beck H, Bornkamm GW, and Conrad M. Loss of thioredoxin reductase 1 renders tumors highly susceptible to pharmacologic glutathione deprivation. *Cancer Res* 70: 9505–9514, 2010.
26. Marzec JM, Christie JD, Reddy SP, Jedlicka AE, Vuong H, Lanken PN, Aplenc R, Yamamoto T, Yamamoto M, Cho HY, and Kleeberger SR. Functional polymorphisms in the transcription factor NRF2 in humans increase the risk of acute lung injury. *FASEB J* 21: 2237–2246, 2007.
27. Meister A. Glutathione metabolism and its selective modification. *J Biol Chem* 263: 17205–17208, 1988.
28. Nakamura T, Nakamura H, Hoshino T, Ueda S, Wada H, and Yodoi J. Redox regulation of lung inflammation by thioredoxin. *Antioxid Redox Signal* 7: 60–71, 2005.
29. Nguyen T, Nioi P, and Pickett CB. The Nrf2-antioxidant response element signaling pathway and its activation by oxidative stress. *J Biol Chem* 284: 13291–13295, 2009.
30. Reddy NM, Kleeberger SR, Kensler TW, Yamamoto M, Hassoun PM, and Reddy SP. Disruption of Nrf2 impairs the resolution of hyperoxia-induced acute lung injury and inflammation in mice. *J Immunol* 182: 7264–7271, 2009.
31. Reddy NM, Potteti HR, Mariani TJ, Biswal S, and Reddy SP. Conditional deletion of Nrf2 in airway epithelium exacerbates acute lung injury and impairs the resolution of inflammation. *Am J Respir Cell Mol Biol* 45: 1161–1168, 2011.
32. Reddy NM, Suryanaraya V, Yates MS, Kleeberger SR, Hassoun PM, Yamamoto M, Liby KT, Sporn MB, Kensler TW, and Reddy SP. The triterpenoid CDDO-imidazolide confers

potent protection against hyperoxic acute lung injury in mice. *Am J Respir Crit Care Med* 180: 867–874, 2009.
33. Rengby O, Cheng Q, Vahter M, Jornvall H, and Arner ES. Highly active dimeric and low-activity tetrameric forms of selenium-containing rat thioredoxin reductase 1. *Free Radic Biol Med* 46: 893–904, 2009.
34. Rhee SG, Chae HZ, and Kim K. Peroxiredoxins: a historical overview and speculative preview of novel mechanisms and emerging concepts in cell signaling. *Free Radic Biol Med* 38: 1543–1552, 2005.
35. Rogers LK, Valentine CJ, Pennell M, Velten M, Britt RD, Dingess K, Zhao X, Welty SE, and Tipple TE. Maternal docosahexaenoic acid supplementation decreases lung inflammation in hyperoxia-exposed newborn mice. *J Nutr* 141: 214–222, 2011.
36. Soini Y, Kahlos K, Napankangas U, Kaarteenaho-Wiik R, Saily M, Koistinen P, Paaakko P, Holmgren A, and Kinnula VL. Widespread expression of thioredoxin and thioredoxin reductase in non-small cell lung carcinoma. *Clin Cancer Res* 7: 1750–1757, 2001.
37. Suvorova ES, Lucas O, Weisend CM, Rollins MF, Merrill GF, Capecchi MR, and Schmidt EE. Cytoprotective Nrf2 pathway is induced in chronically txnrd 1-deficient hepatocytes. *PloS One* 4: e6158, 2009.
38. Tipple TE, Welty SE, Rogers LK, Hansen TN, Choi YE, Kehrer JP, and Smith CV. Thioredoxin-related mechanisms in hyperoxic lung injury in mice. *Am J Respir Cell Mol Biol* 37: 405–413, 2007.
39. Yates MS, Tauchi M, Katsuoka F, Flanders KC, Liby KT, Honda T, Gribble GW, Johnson DA, Johnson JA, Burton NC, Guilarte TR, Yamamoto M, Sporn MB, and Kensler TW. Pharmacodynamic characterization of chemopreventive triterpenoids as exceptionally potent inducers of Nrf2-regulated genes. *Mol Cancer Therapeut* 6: 154–162, 2007.
40. Yoo MH, Xu XM, Carlson BA, Gladyshev VN, and Hatfield DL. Thioredoxin reductase 1 deficiency reverses tumor phenotype and tumorigenicity of lung carcinoma cells. *J Biol Chem* 281: 13005–13008, 2006.

Address correspondence to:
Dr. Trent E. Tipple
Center for Perinatal Research, W211
The Research Institute at Nationwide Children's Hospital
700 Children's Drive
Columbus, OH 43205

E-mail: trent.tipple@nationwidechildrens.org

Date of first submission to ARS Central, October 28, 2011; date of final revised submission, May 17, 2012; date of acceptance, May 18, 2012.

Abbreviations Used

AFN = auranofin
ANOVA = analysis of variance
ARDS = acute respiratory distress syndrome
ARE = antioxidant response element
ATG = aurothioglucose
BPD = bronchopulmonary dysplasia
BSO = buthionine sulfoximine
CDDO = 2-cyano-3,12-dioxooleana-1,9(11)-dien-28-oyl
DAB = diaminobenzamidine
DNCB = dinitrochlorobenzene
DTT = dithiotreitol
EDTA = ethylenediaminetetracetic acid
GCLM = glutamate-cysteine ligase modifier subunit
GSH = glutathione
i.p. = intraperitoneal
H_2O_2 = hydrogen peroxide
HO-1 = heme oxygenase 1
Keap1 = Kelch ECH associating protein-1
LDH = lactate dehydrogenase
mtCC = murine transformed Clara cells
NADH = nicotinamide adenine dinucleotide
NADPH = nicotinamide adenine dinucleotide phosphate
NQO1 = NADPH:quinone oxidoreductase 1
Nrf2 = nuclear factor E2-related factor 2
PCR = polymerase chain reaction
PMSF = phenylmethylsulfonyl fluoride
qRT-PCR = quantitative reverse transcriptase–PCR
RA = room air
RSV = respiratory syncytial virus
Sec = selenocysteine
SEM = standard error of the mean
SFN = sulforaphane
TBS-T = tris-buffered saline with 1% Tween 20
Trx1 = thioredoxin-1
TrxR1 = thioredoxin reductase-1